Composites: Part B 51 (2013) 19–27

Contents lists available at SciVerse ScienceDirect

Composites: Part B

journal homepage: www.elsevier.com/locate/compositesb

Design limits for RC slabs strengthened with hybrid FRP–HPC retrofit system

Jung J. Kim [a], Hyuk-Chun Noh [a], Mahmoud M. Reda Taha [b], Ayman Mosallam [c,*]

[a] Dept. of Civil and Environmental Engineering, Sejong University, Seoul 143-747, Republic of Korea
[b] Dept. of Civil Engineering, University of New Mexico, MSC01 1070, 1 University of New Mexico, NM 87131-0001, USA
[c] Dept. of Civil Engineering, University of California, Irvine, CA 92697-2175, USA

ARTICLE INFO

Article history:
Received 13 October 2012
Received in revised form 26 December 2012
Accepted 26 December 2012
Available online 22 February 2013

Keywords:
A. Carbon-carbon composites (CCCs)
B. Strength
C. Analytical Modeling
Repair and retrofit

ABSTRACT

A polymeric hybrid composite system made of high-performance concrete (HPC) and an innovative carbon/epoxy reinforced polymer (CFRP) unidirectional laminates was proposed as a retrofit system to enhance flexural strength and ductility of reinforced concrete (RC) slabs. The effectiveness of the proposed system was confirmed through experimental evaluation of three full-scale one-way slabs having two continuous spans. In this study, the results of the loading tests for the hybrid high-performance retrofit system are presented and discussed. Design limits to derive a flexural failure of a continuous RC slab strengthened with the hybrid retrofit system are extracted. Using the proposed design limits, the procedure of a flexural failure design for a continuous RC slab strengthened with the hybrid retrofit system is demonstrated with numerical examples for two types of the retrofit systems with respect to overlay strength. The flexural failure design limits can be extended for flexural and shear strengthening design with externally bonded FRP to ensure flexure failure for a continuous flexural members.

1. Introduction

Aging of infrastructures due to limited maintenance and load increase necessitate rehabilitation. Strengthening of infrastructures is also necessary to resist unexpected excessive loading [1–3]. Steel and fiber reinforced polymer (FRP) composite plates have been used to enhance flexural capacity of reinforced concrete (RC) structures by externally attaching these plates to the tension zone of RC structures [4]. FRP composite systems proved to be a viable and economical alternative due to their high strength-to-weight ratio (specific strength), ease of application and for being corrosion resistant [5,6]. While FRP material can resist compressive stresses, there are some potential concerns such as micro-buckling of fibers that needs to be addressed when a composite laminate is exposed to compression [7]. Conventionally, FRP laminates are installed at the top and the underside of an existing floor slab to enhance moment capacities of negative sections, "N-N" section in Fig. 1a and positive sections, "P-P" section in Fig. 1a, respectively. Installing FRP at the top of the slab can be typically performed without much difficulty. However, in most cases there are many obstacles to access the underside of the slab (anti-gravity applications) such as suppression system, electrical wiring and ventilation ducts. This also applies to retrofitting bridge overpasses where traffic interruption in the road below is unavoidable or a special shoring system is required for bridges crossing over waterways. Moreover, additional anchoring systems might be necessary to hold FRP laminates in place during initial curing of the adhesive, which makes it further difficult to apply the FRP to the underside of slab or bridge deck. Such obstacles increase the cost of rehabilitation of strengthening of the slab significantly.

This research work suggests the use of an innovative hybrid system composed of high-performance polymeric concrete (HPC) and carbon/epoxy fiber reinforced polymer (CFRP) unidirectional laminates as an effective retrofit methodology to improve the strength and ductility of existing continuous reinforced concrete (RC) slabs by installing the hybrid FRP system only to the top of the slab [8] as shown in Fig. 1b. Three one-way RC slabs with two continuous spans of 1219 mm wide and 2438 mm long were tested to examine the proposed system ability to enhance the moment capacity of the slab. One slab was used as a reference slab and the other two slabs were strengthened with the proposed retrofit system with two types of HPC with compressive strength of 69 MPa and 97 MPa. Full-scale experimental results indicated that the proposed system can increase the ultimate load capacity and ductility of the retrofitted RC slabs by about 164% and 122%, respectively, as compared with the reference "as-built" slab [8]. The slabs retrofitted with the proposed hybrid system failed in shear as shown in Fig. 2a while the control slab failed by consisting plastic hinges as shown in Fig. 2b [8]. While this sudden failure was initiated by CFRP laminate debonding from the concrete slab, shear failure was predicted to govern if perfect bond is assumed. Shear failure would stem from the excessive enhancement of the flexural strength over the

* Corresponding author. Tel.: +1 949 824 3369; fax: +1 949 824 2117.
E-mail address: mosallam@uci.edu (A. Mosallam).

1359-8368/$ - see front matter © 2013 Elsevier Ltd. All rights reserved.
http://dx.doi.org/10.1016/j.compositesb.2012.12.012

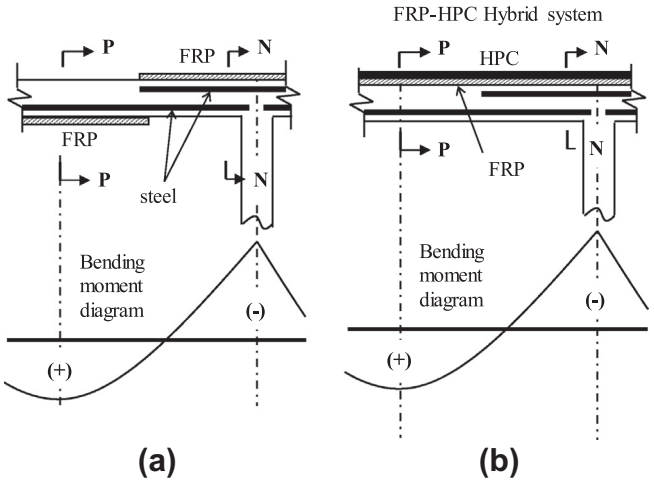

Fig. 1. Flexural strengthening of continuous RC slabs using (a) conventional bonded FRP system and (b) proposed hybrid FRP–HPC system with respect to the design moment diagram.

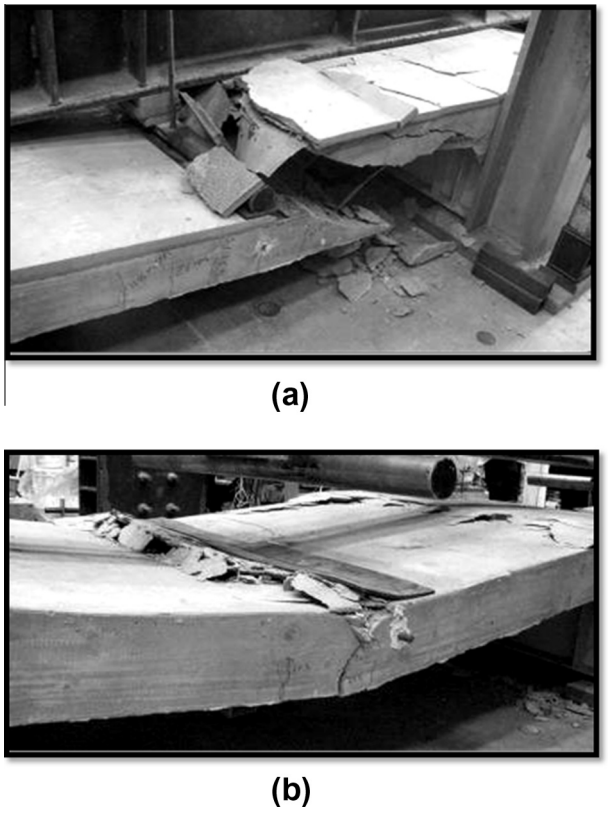

Fig. 2. Failure shapes of (a) the retrofitted slabs with the hybrid high-performance composite system and (b) the control slab [8].

shear strength. Therefore, a design methodology is necessary for the practical use of the hybrid system to retrofit continuous RC slabs. In order to ensure ductile failure of RC flexural members, the shear strength should be equal or greater than the flexural strength at all sections of the RC member in order to prevent the sudden and brittle shear failure [9].

In this paper, flexural failure design-limit state of a continuous RC slab according to its moment and shear carrying capacities are extracted and used to develop a design methodology of the proposed hybrid FRP–HPC retrofitting system. This design methodology is illustrated using design examples.

2. Flexural failure limits

When a flexural member is a part of a frame, the bending moment distributions along the member depend on the flexural rigidities of the flexural member and the columns of that frame. Therefore, the moment at a section of the flexural member, which has the length l and is subjected to a uniform distributed load w, can be expressed as $M = Cwl^2$, where the coefficient C is related to the flexural rigidities of the corresponding frame members. If infinite rigidity of columns is considered, C will be 1/12, which is for the fixed end moment of a flexural member subjected to a uniform distributed load w. For a practical design purpose, ACI 318M-08 proposed moment and shear coefficients with the factored distributed load as shown in Fig. 3 for column support case.

Considering a flexural member having symmetric boundary conditions, which is comparable to the interior span in Fig. 3, one can formulate the limits for failure modes considering the relationship between the moment carrying capacity of $M_{n,N}$ and $M_{n,P}$ at the support (negative moment) and the mid-span (positive moment) sections respectively and the shear carrying capacity V_n of the slab sections. The moment limits can be established as a function of the shear limits as follow:

$$M_{n,N} = \frac{2C_{m,N}}{C_v} V_n l_n \tag{1}$$

$$M_{n,P} = \frac{2C_{m,P}}{C_v} V_n l_n \tag{2}$$

where $M_{n,N}$ is the moment carrying capacity of the support section (negative moment); $M_{n,P}$ is the moment carrying capacity of the mid-span section (positive moment); V_n is the shear carrying capacity of the slab sections; $C_{m,N}$ is the moment coefficient for negative moment; $C_{m,P}$ is the moment coefficient for positive moment; C_v is the shear coefficient for support sections; and l_n is the net span length between support columns.

Here, the absolute values of the moment coefficients are considered since the signs are used only to indicate moment directions (refer to Fig. 3.) As shown in Fig. 4, the limits of Eqs. (1) and (2) can be depicted with a given shear carrying capacity, V_n, and the moment and the shear coefficients. The different regions in Fig. 4 can be analyzed as follows.

Region I: This region, where $M_{n,P} < 2C_{m,P}V_n l_n/C_v$ and $M_{n,N} < 2C_{m,N}V_n l_n/C_v$, shown in Fig. 4 includes a balanced flexural failure, where the sections at the support and at the mid-span fail simultaneously as the applied load reaches its ultimate value w_u. This failure mode occurs when the condition in Eq. (3) is satisfied.

$$\frac{M_{n,N}}{M_{n,P}} = \frac{C_{m,N}}{C_{m,P}} \quad \text{for Region I in Fig.4} \tag{3}$$

When the left hand-side term appears in Eq. (3) is less than the right hand-side term, the failure mechanism will occur by forming the first plastic hinges at the support sections and the ultimate slab failure will occur once another plastic hinge is formed at the mid-span section as shown in Fig. 5. This failure mode is named "D-1" and represents the most conventional failure mode for continuous RC slabs as the left hand-side term in Eq. (3) is usually designed such that it is slightly higher than or equal to 1.0, while the right hand-side term of the equation is taken equal to 1.45 for the interior span design as illustrated in Fig. 3. When the left hand-side term in Eq. (3) is higher than the right hand-side term of the equation, a plastic hinge is developed at the mid-span section first and the ultimate failure of the slab will occur upon the development of additional plastic hinges at the support sections as shown in Fig. 6.

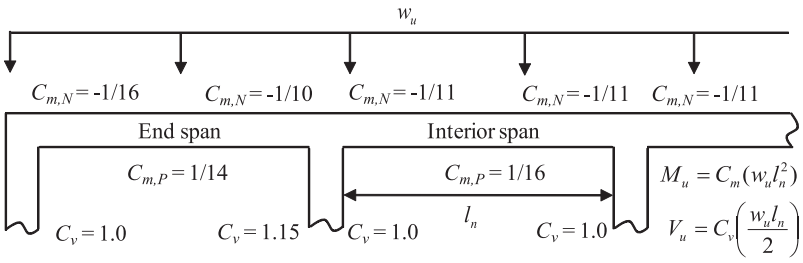

Fig. 3. Example for the moment and shear coefficients proposed by ACI 318M-08 [10] for continuous slab design with the factored distributed load.

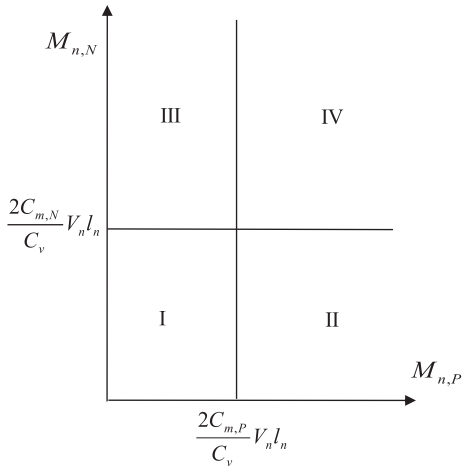

Fig. 4. The failure regions according to the relationship between the moment carrying and shear carrying capacity of the RC slab section.

This failure mode is named as "D-2". These two failure modes represent ductile flexural failure modes and both are located at Region I in Fig. 4. To achieve D-1 and D-2 failure modes, the shear failure shall be prevented and the limits of $M_{n,N}$ and $M_{n,P}$ according to V_n can be designed for D-1 and D-2 failure modes.

Regions II & III: For Regions II and III in Fig. 4, either flexural failure only or a combination of the flexural and shear failures at the slab sections can occur. In Region II, the two conditions $M_{n,P} > 2C_{m,P}V_n l_n/C_v$ and $M_{n,N} < 2C_{m,N}V_n l_n/C_v$ apply. Thus the support sections fail first and form plastic hinges as shown in Fig. 5a or Fig. 7a at the amount of the applied load,

$$w_{u1} = \frac{M_{n,N}}{C_{m,N} l_n^2} \tag{4}$$

Forming these plastic hinges at the supports converts the statically indeterminate RC slab to a statically determinate simple beam subjected to $M_{n,N}$ at the supports. Consequently, the mid-span section is subjected to the moment of $M_P = C_{m,P} w_{u1} l_n^2$ and the support sections are subjected to the shear force of $V_N = C_v(w_{u1} l_n/2)$. The load carrying capacity of the RC slab is then governed by either the additional moment at the mid-span section or the additional shear force at the support sections. If the load carrying capacity of the RC slab is governed by the additional moment at the mid-span section as shown in Fig. 5b, the additional distributed load capacity w_{u2}^M can be estimated by considering the remaining flexural moment carrying capacity of the mid-span section, $(M_{n,P} - M_P)$ as:

$$w_{u2}^M = \frac{8(M_{n,P} - M_P)}{l_n^2} \tag{5}$$

For this case, the slab will fail by forming three plastic hinges, two at the support sections and one at the mid-span section. If the load carrying capacity of the RC slab is governed by the additional shear force at the support sections as shown in Fig. 7b, the additional distributed load w_{u2}^V can be estimated by considering the remaining shear carrying capacity of the support sections, $(V_{n,N} - V_N)$ as

$$w_{u2}^V = \frac{2(V_{n,N} - V_N)}{l_n} \tag{6}$$

For this case, the slab will fail by shear after forming only two plastic hinges at the support sections. The design limit is then formulated as

$$w_{u2}^M = w_{u2}^V \tag{7}$$

If w_{u2}^M is less than w_{u2}^V, the failure mode will be D-1 in Fig. 5. If w_{u2}^M is higher than w_{u2}^V, the slab will fail by shear after forming two plastic hinges at the support sections. This failure mode is named "DB-1"

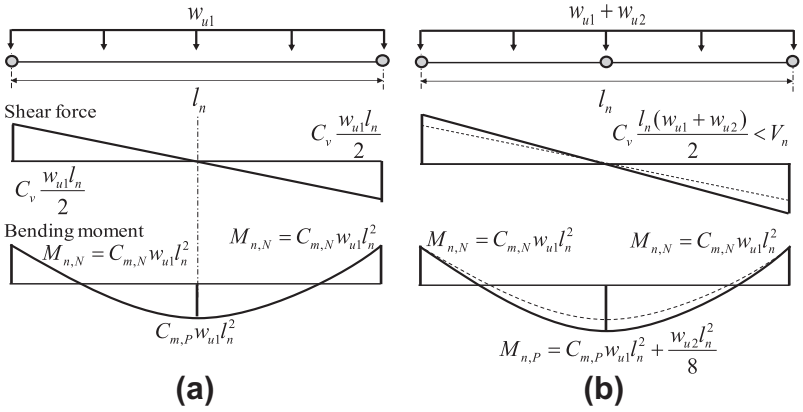

Fig. 5. Description of failure mechanism for D-1 failure mode, (a) flexural failure at the support sections first and then and (b) flexural failure at the mid-span section.

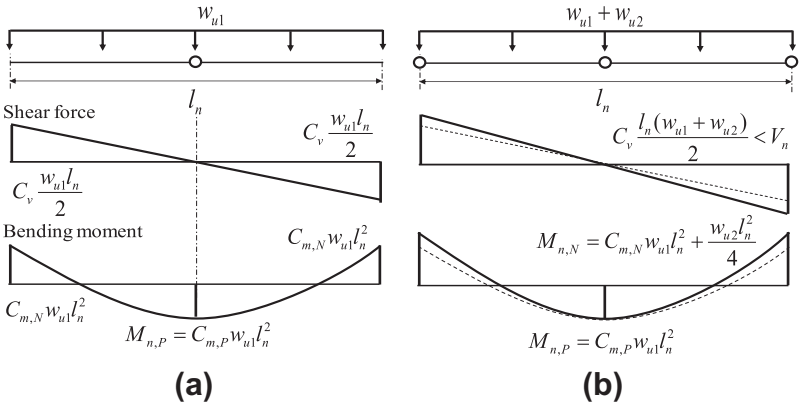

Fig. 6. Description of failure mechanism for D-2 failure mode, (a) flexural failure at the mid-span section first and then (b) flexural failure at the support sections.

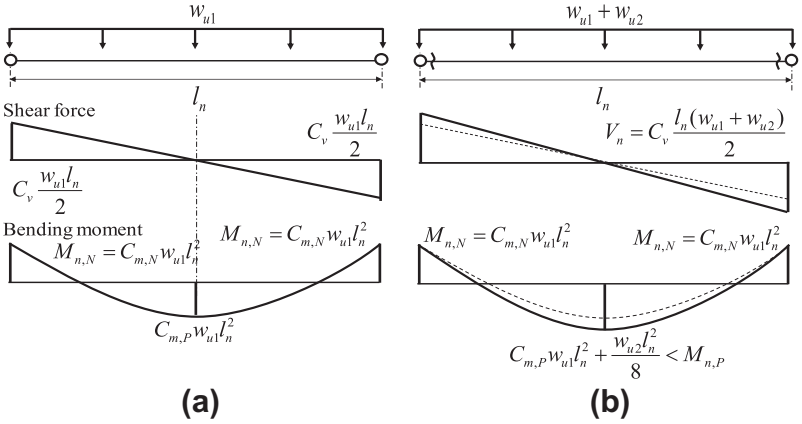

Fig. 7. Description of failure mechanism for DB-1 failure mode, (a) flexural failure at the support sections first and then (b) shear failure at the support sections.

and is shown in Fig. 7. By using M_p and V_N in Eqs. (5) and (6) and using the design limit in Eq. (7), one can find

$$M_{n,N}\left(\frac{C_v/8 - C_{m,P}}{C_{m,N}}\right) + M_{n,P} = \frac{1}{4} V_n l_n \quad \text{for Region II in Fig.4} \tag{8}$$

At Region III, where $M_{n,P} < 2C_{m,P}V_n l_n/C_v$ and $M_{n,N} > 2C_{m,N}V_n l_n/C_v$, the mid-span section fails first and forms a plastic hinge as shown in Fig. 6a or Fig. 8a thus:

$$w_{u1} = \frac{M_{n,P}}{C_{m,P} l_n^2} \tag{9}$$

After mid-span failure, the mid-span cannot take anymore load and hold the moment $M_{n,P}$. At this time, the support sections are subjected to the moment of $M_N = C_{m,N} w_{u1} l_n^2$ and the shear force of $V_N = C_v(w_{u1} l_n/2)$. If the load carrying capacity of the RC slab is governed by the additional moment at the support sections as shown in Fig. 6b, the additional distributed load can be estimated by considering the remaining flexural moment carrying capacity of the support sections, $(M_{n,N} - M_N)$ as:

$$w_{u2}^M = \frac{4(M_{n,N} - M_N)}{l_n^2} \tag{10}$$

If the load carrying capacity of the RC slab is governed by the additional shear force at the support sections as shown in Fig. 8b, the additional distributed load is calculated as in Eq. (6) which is repeated here:

$$w_{u2}^V = \frac{2(V_{n,N} - V_N)}{l_n} \tag{6}$$

If w_{u2}^M in Eq. (10) is less than w_{u2}^V, the failure mode will be D-2 descried in Fig. 6 while w_{u2}^M in Eq. (10) is higher than w_{u2}^V, the slab will fail in shear after forming one plastic hinge at the mid-span section. This failure mode is named as "DB-2" and is shown in Fig. 8. Now, considering the design limit in Eq. (7) with Eqs. (6) and (10), the design limit at Region III can be derived as follows:

$$M_{n,N} + \left(\frac{C_v/4 - C_{m,N}}{C_{m,P}}\right) M_{n,P} = \frac{1}{2} V_n l_n \quad \text{for Region III in Fig.4} \tag{11}$$

Region IV: At Region IV in Fig. 4, where $M_{n,P} > 2C_{m,P}V_n l_n/C_v$ and $M_{n,N} > 2C_{m,N}V_n l_n/C_v$, the slab will fail in shear without forming any plastic hinge as shown in Fig. 9. This failure mode is named B-1. The limit equations in each region of Fig. 4 are depicted in Fig. 10 and the failure modes are summarized in Table 1. The last three failure modes DB-1, DB-2 and B-1 represent brittle shear failure and thus might not be preferable for design. Therefore, when an existing slab can be classified to fail in mode D-1, one might design the strengthening system to also fail in modes D-1 or D-2 to avoid brittle shear failure.

For failure modes of D-1 and D-2, the failure loads can be calculated as:

$$w_f = \phi_m \frac{8}{l_n^2}\left(M_{n,P} + M_{n,N}\frac{(1 - 8C_{m,P})}{8C_{m,N}}\right) \quad \text{Failure mode D-1} \tag{12}$$

$$w_f = \phi_m \frac{4}{l_n^2}\left(M_{n,N} + M_{n,P}\frac{(1 - 4C_{m,N})}{4C_{m,P}}\right) \quad \text{Failure mode D-2} \tag{13}$$

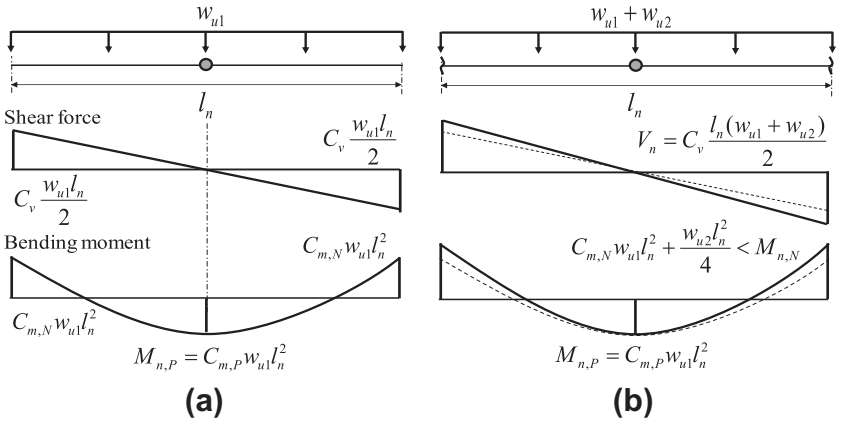

Fig. 8. Description of failure mechanism for DB-2 failure mode, (a) flexural failure at the mid-span section first and then (b) shear failure at the support sections.

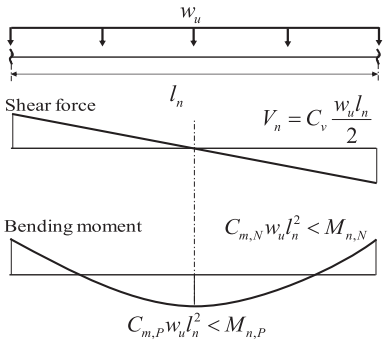

Fig. 9. Description of failure mechanism for B-1, shear failure.

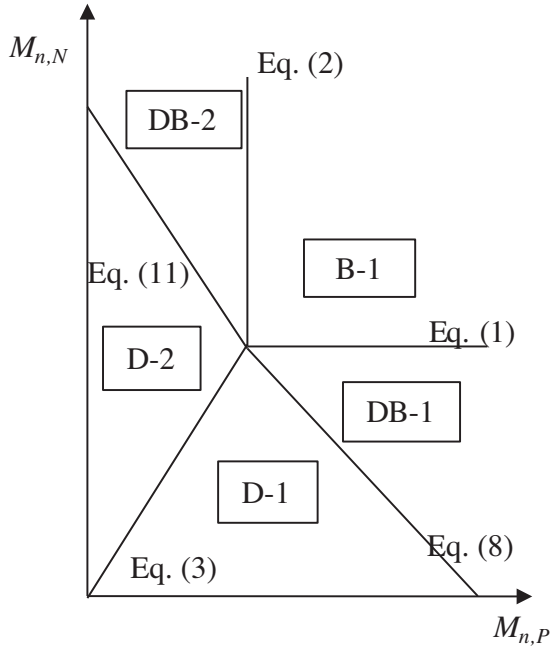

Fig. 10. Failure modes according to $M_{n,N}$, $M_{n,P}$ and V_n of a RC slab.

For failure modes of DB-1, DB-2 and B-1, the failure loads can be calculated as:

$$w_f = \phi_v \frac{2V_n}{C_v l_n} \quad \text{Failure modes DB-1, DB-2 and B-1} \tag{14}$$

Table 1
Summary of the failure modes according to $M_{n,N}$, $M_{n,P}$ and V_n of the slabs.

Failure modes	First plastic hinge	Second plastic hinge	Shear failure	Failure type
D-1	Support	Mid-span	–	Ductile
D-2	Mid-span	Support	–	Ductile
DB-1	Support	–	Support	Brittle
DB-2	Mid-span	–	Support	Brittle
B-1	–	–	Support	Brittle

where ϕ_m and ϕ_v are strength reduction factors for the flexural strength and the shear strength respectively provided in design specifications such as ACI 318-08 [10].

3. Design examples

For design examples of the proposed retrofit system, moment and shear coefficients proposed in ACI 318M-08 [10] are considered as shown in Fig. 3 for the interior span of column support case, where $C_{m,N}$ = 1/11, $C_{m,P}$ = 1/16, C_v = 1.0. Similar slab dimensions for the validation of the hybrid retrofit system [8] are also considered. Slab dimensions and material properties are presented in Table 2. The mechanical properties of two types of the hybrid retrofit system which consists of CFRP and HPC, S-1 and S-2 system according to HPC overlay types, are presented in Table 3. The slab is analyzed in Table 4 and the failure modes are defined by generating the corresponding limits for different failure modes and the status of the moment carrying capacities as shown in Fig. 11. Based on the external FRP design procedure proposed by ACI 440 committee [7], additional requirements are checked and applied for the design of the hybrid retrofit system. Long term effect under service load is not considered here. The thickness of CFRP is assumed as a design variable and the optimal thickness to ensure ductile flexural failure is identified. Strength reduction factors of 0.9 and 0.75 are used for the flexural strength and shear strength respectively as per ACI codes. The detailed design procedure is presented in Tables 5 and 6 for S-1 and S-2 systems. The portion of the moment capacity generated by CFRP is reduced by reliability factor of 0.85 following ACI 440 recommendation [7]. Although the debonding failure strain of CFRP and the reliability factor for CFRP debonding are considered for the design procedure, shear anchors for CFRP and HPC shall be provided to maintain the retrofitted slab integrity. The details for the necessary anchoring area and FRP development length to prevent concrete cover delamination with FRP can be found elsewhere [11,12].

Table 2
Slab dimensions and properties for design example of the proposed retrofit system.

Section	l_n (mm)	h (mm)	A_s (mm^2/m)	D (mm)	A_{sc} (mm^2/m)	d_c (mm)	f'_c (MPa)	γ_c (kg/m^3)	f_y (MPa)	E_s (GPa)
Support	2438.4	152.4	635	127	635	25.4	20.7	2400	410	200
Mid-span					–	–				

Table 3
Mechanical properties of the materials used in the hybrid retrofit systems [8].

System	HPC			CFRP			
	Description	t_H (mm)	f'_H (MPa)	t_F (mm)	f_{cF} (MPa)	f_{tF} (MPa)	E_F (GPa)
S-1	Polymer concrete	24.4	69	1	500	1170	72.6
S-2	Epoxy/mortar	24.4	97.2				

Table 4
Analysis of the slab for design examples per unit width (1 m).

Analysis	Existing slab
ACI moment and shear coefficient for interior span with column support [10] (absolute values)	$C_{m,N}$ = 1/11, C_{mP} = 1/16, and C_v = 1.0
Factored section capacity	$\phi_f M_{n,P}$ = 28 kN m, $\phi_f M_{n,N}$ = 28.5 kN m, $\phi_v V_n$ = 72.2 kN
Designed factored load	
$w_u = \min(w_{u,P}, w_{u,N}, w_{u,V})$	w_u = min(75.3, 52.7, 59.2) = 52.7 kN/m
$w_{u,P} = \frac{\phi_f M_{n,P}}{C_{m,P} l_n^2}$	$w_{u,P} = \frac{28}{(1/16)(2.4384)^2} = 75.3$ kN/m
$w_{u,N} = \frac{\phi_f M_{n,N}}{C_{m,N} l_n^2}$	$w_{u,N} = \frac{28.5}{(1/11)(2.4384)^2} = 52.7$ kN/m
$w_{u,V} = \frac{2\phi_v V_n}{C_v l_n}$	$w_{u,V} = \frac{2(72.2)}{(1)(2.4384)} = 59.2$ kN/m
Failure mode	DB-1 as shown in Fig. 10
Failure load Eq. (11) for Mode III	$w_f = \frac{2(72.2)}{(1)(2.4384)} = 59.2$ kN/m
Preliminary calculations for retrofit design	
Self-weight $w_D = \gamma_c bh$	$w_D = (2400 \times 9.8 \times 10^{-3})(1)(0.1524) = 3.58$ N/mm
Support $M_{D,N} = C_{m,N}(w_D l_n^2)$	$M_{D,N} = (1/11)(3.58 \times 2438.4^2)/1000 = 1935.1$ kN- mm
$E_c = 4700\sqrt{f'_c}$	$E_c = 4700\sqrt{20.7} = 21400$ MPa
Support $I_{cr,N}$	$I_{cr} = 69.3 \times 10^6$ mm^4
Support $c_N = kd$	c_N = 21.7 mm

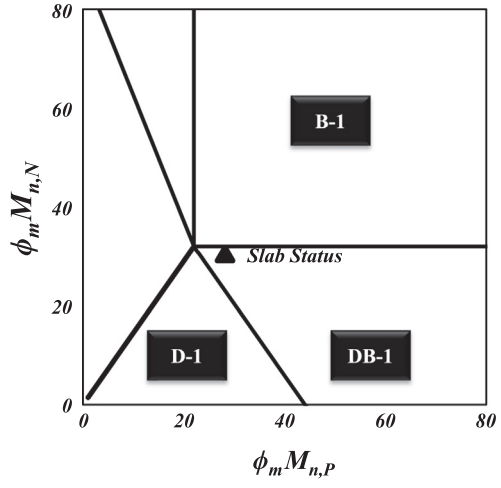

Fig. 11. The formulated failure limits and the estimated status of moment carrying capacities for the design example slab.

4. Results and discussions

For the analysis of the slab considered in the design example presented in Table 4, the factored design load w_u is determined as 52.7 kN/m. The failure mode of the slab is also expected as DB-1 failure mode with the ultimate load, w_f, of 59.2 kN/m. Therefore, it is noticeable one can see that although the flexural strengths at critical sections (mid-span section and support section) of the slab are designed to be less than the corresponding shear strength, there is a chance that the slab fails in shear when the flexural failure limits are considered (refer to Fig. 11) For the first iteration of the design procedure in Table 5, the CFRP laminate thickness for S-1 and S-2 systems was initially assumed to be 1 mm. The CFRP laminate thickness was then adjusted to ensure the occurrence of ductile flexural failure. The final iteration of the design procedure with the adjusted CFRP ply thickness is presented in Table 6. In step 2 of Table 5, the compressive strength of HPC overlay is checked to ensure the CFRP laminate at the mid-span is subjected to tensile stresses [8]. The analysis shows that the concrete with relatively low compressive strength can be used as an overlay to induce tension in CFRP laminate applied at the mid-span. However, the use of high-strength concrete is preferred in order to prevent any potential shear failure of the overlay and to increase the flexural strength of the slab at the mid-span. The environmental reduction factor for CFRP laminates [7] indicated in step 3 was not considered as the CFRP is covered by HPC overlay and is not exposed to the outside environment. The existing state of strain [7] at step 4 is considered only for the support section as

Table 5
The first iteration of design examples per unit width (1 m).

Procedure	S-1 system	S-2 system
24.4 mm Thick HPC overlay	$f'_H = 69$ MPa	$f'_H = 97.2$ MPa
1. CFRP thickness estimation	CFRP thickness, $t_F = 1$ mm	
2. Check HPC strength is large enough to generate tension in CFRP at mid-span section [8]	$f'_H \geqslant \frac{0.003(72{,}600)}{1.445}\left(\frac{1.0}{24.4}\right)^2 + \frac{410(0.635)}{0.7225(24.4)} = 15$ MPa $f'_H \geqslant 0.15(20.7) + \frac{0.003(72{,}600)}{1.7}\left(\frac{1.0}{24.4}\right)^2 + \frac{410(0.635)}{0.85(24.4)} = 15.9$ MPa O.K. for both system	
3. Environmental reduction factor for the ultimate strength and strain of CFRP [7], C_E	C_E is equal to 1 for the proposed retrofit system as CFRP is overlaid by HPC $f_{fu} = 1170$ MPa, $\varepsilon_{fu} = 0.016$ from Table 3	
4. Existing state of strain at support [7] $\varepsilon_{bi} = \frac{M_D(d_f - kd)}{I_{cr}E_c}$	kd is c_N in Table 4 and d_f is the slab height for the proposed retrofit system $\varepsilon_{bi} = \frac{(1.935\times10^6)(152.4-21.7)}{(69.3\times10^6)(21{,}400)} = 0.00017$	
5. Design strain of CFRP [7]	$\varepsilon_{fd} = 0.41\sqrt{\frac{20.7}{(1)(72{,}600)(1)}} = 0.0069 \leqslant 0.9(0.016) = 0.0144$	
6. Concrete strain at failure	$\varepsilon_{cu} = 0.003$	$\varepsilon_{cu} = 0.003$
7. Neutral axis depth for support section, c_N mid-span section, c_P	$c_N = 48.6$ mm $c_P = 10.9$ mm	$c_N = 48.6$ mm $c_P = 9.1$ mm
8. Check FRP strain at support section $\varepsilon_{fe,N} = \varepsilon_{cu}\left(\frac{h-c_N}{c_N}\right) - \varepsilon_{bi} \leqslant \varepsilon_{fd}$ and mid-span section $\varepsilon_{fe,P} = \varepsilon_{cu}\left(\frac{t_H-c_P}{c_P}\right) \leqslant \varepsilon_{fd}$ $^*\varepsilon_{bi}$ for mid-span section is equal to zero	support section $\varepsilon_{fe,N} = 0.003\left(\frac{152.4-48.6}{48.6}\right) - 0.00017 = 0.00623 < 0.0069$ mid-span section $\varepsilon_{fe,P} = 0.003\left(\frac{24.4-10.9}{10.9}\right) = 0.0037 < 0.0069$ Both are O.K. use $\varepsilon_{cu} = 0.003$	support section $\varepsilon_{fe,N} = 0.003\left(\frac{152.4-48.6}{48.6}\right) - 0.00017 = 0.00623 < 0.0069$ mid-span section $\varepsilon_{fe,P} = 0.003\left(\frac{24.4-9.1}{9.1}\right) = 0.005 < 0.0069$ Both are O.K. use $\varepsilon_{cu} = 0.003$
9. Check tension steel strain at support section $\varepsilon_{s,N} = \varepsilon_{cu}\left(\frac{d-c_N}{c_N}\right)$ and mid-span section $\varepsilon_{s,P} = \varepsilon_{cu}\left(\frac{d+t_H+t_F-c_P}{c_P}\right)$	support section $\varepsilon_{s,N} = 0.003\left(\frac{127-48.6}{48.6}\right) = 0.0048 > 0.002$ yield mid-span section $\varepsilon_{s,P} = 0.003\left(\frac{127+24.4+1.0-10.9}{10.9}\right) = 0.0389 > 0.002$ yield	support section $\varepsilon_{s,N} = 0.003\left(\frac{127-48.6}{48.6}\right) = 0.0048 > 0.002$ yield mid-span section $\varepsilon_{s,P} = 0.003\left(\frac{127+24.4+1.0-9.1}{9.1}\right) = 0.0472 > 0.002$ yield
10. Flexural strength at support section Steel contribution $M_{n,Ns} = A_s f_y\left(d - \frac{\beta_1 c_N}{2}\right)$ CFRP contribution $M_{n,NF} = t_F b E_F \varepsilon_{fe,N}\left(h - \frac{\beta_1 c_N}{2}\right)$	$M_{n,Ns} = \frac{635(410)}{10^6}\left(127 - \frac{0.85(48.6)}{2}\right) = 27.6$ kN m $M_{n,NF} = \frac{(1)(1000)(72{,}600)(0.00623)}{10^6}\left(152.4 - \frac{0.85(48.6)}{2}\right) = 59.5$ kN m	$M_{n,Ns} = \frac{635(410)}{10^6}\left(127 - \frac{0.85(48.6)}{2}\right) = 27.6$ kN m $M_{n,NF} = \frac{(1)(1000)(72{,}600)(0.00623)}{10^6}\left(152.4 - \frac{0.85(48.6)}{2}\right) = 59.5$ kN m
11. Flexural strength at mid-span section Steel contribution $M_{n,Ps} = A_s f_y\left(d + t_H + t_F - \frac{\beta_1 c_P}{2}\right)$ CFRP contribution $M_{n,NF} = t_F b E_F \varepsilon_{fe,P}\left(t_H - \frac{\beta_1 c_P}{2}\right)$	$M_{n,Ps} = \frac{635(410)}{10^6}\left(127 + 24.4 + 1.0 - \frac{0.85(10.9)}{2}\right) = 38.4$ kN m $M_{n,PF} = \frac{(1)(1000)(72{,}600)(0.0037)}{10^6}\left(24.4 - \frac{0.85(10.9)}{2}\right) = 5.3$ kN m	$M_{n,Ps} = \frac{635(410)}{10^6}\left(127 + 24.4 + 1.0 - \frac{0.85(9.1)}{2}\right) = 38.6$ kN m $M_{n,PF} = \frac{(1)(1000)(72{,}600)(0.005)}{10^6}\left(24.4 - \frac{0.85(9.1)}{2}\right) = 7.4$ kN m
12. Factored flexural section capacity $\phi_f M_n = \phi_f(M_{ns} + \psi_f M_{nF})$ $\phi_f = 0.9$, $\psi_f = 0.85$	support section $\phi_f M_{n,N} = 0.9[27.6 + 0.85(59.5)] = 70.3$ kN m mid-span section $\phi_f M_{n,P} = 0.9[38.4 + 0.85(5.3)] = 38.6$ kN m	Support section $\phi_f M_{n,N} = 0.9[27.6 + 0.85(59.5)] = 70.3$ kN m mid-span section $\phi_f M_{n,P} = 0.9[38.6 + 0.85(7.4)] = 40.4$ kN m
13. Factored shear carrying capacity $\phi_v V_n = \phi_v\left(d\sqrt{f'_c} + t_H\sqrt{f'_H}\right)\frac{b}{6}$ $\phi_v = 0.75$	$\phi_v V_n = \frac{0.75}{6}\left(127\sqrt{20.7} + 24.4\sqrt{69}\right) = 97.5$ kN	$\phi_v V_n = \frac{0.75}{6}\left(127\sqrt{20.7} + 24.4\sqrt{97.2}\right) = 102.2$ kN
14. Design factored load $w_u = \min(w_{u,P}, w_{u,N}, w_{u,V})$ $w_{u,P} = \frac{\phi_f M_{n,P}}{C_{m,P} l_n^2}$ $w_{u,N} = \frac{\phi_f M_{n,N}}{C_{m,N} l_n^2}$ $w_{u,V} = \frac{2\phi_v V_n}{C_v l_n}$	$w_u = 79.9$ kN/m $w_{u,P} = \frac{38.6}{(1/16)(2.4384)^2} = 103.8$ kN/m $w_{u,N} = 130$ kN/m $w_{u,V} = \frac{2(97.5)}{(1)(2.4384)} = 79.9$ kN/m	$w_u = 83.8$ kN/m $w_{u,P} = \frac{40.4}{(1/16)(2.4384)^2} = 108.7$ kN/m $w_{u,N} = 130$ kN/m $w_{u,V} = \frac{2(102.2)}{(1)(2.4384)} = 83.8$ kN/m
15. Failure mode	The failure mode is B-1 as shown in Fig. 12a	The failure mode is B-1 as shown in Fig. 12b
16. Failure load Eq. (14) for B-1	$w_f = \frac{2(97.5)}{(1)(2.4384)} = 79.9$ kN/m	$w_f = \frac{2(102.2)}{(1)(2.4384)} = 83.8$ kN/m

the CFRP is installed at the compression zone of the slab for the mid-span section. The debonding failure strain of CFRP [7] is calculated at step 5 and is used in steps 6 through 8 to check that concrete strain can reach the failure strain of 0.003 before debonding of CFRP occurs. If CFRP debonding occurs before the concrete strain reaches the failure strain, the strain compatibility condition is rear-

Table 6
Final iteration of design examples after adjusting CFRP thickness to derive ductile flexural failure per unit width (1 m).

Procedure	S-1 system	S-2 system
1. CFRP thickness estimation (steps 1 through 15 were repeated) adjust t_F until the left term of Eqs. (8), (11) is less than the corresponding right term	t_F = 0.13 mm	t_F = 0.18 mm
Steps 2 through 5 are same	It is not necessary to do step 2 again when t_F decreases	
6. Concrete strain at failure Adjust until force equilibrium is satisfied (steps 6 through 9 were repeated)	ε_{cu} = 0.00117	ε_{cu} = 0.00126
7. Neutral axis depth	c_N = 21.9 mm c_P = 5.9 mm	c_N = 23.5 mm c_P = 4.7 mm
8. Check FRP strain	$\varepsilon_{fe,N} = 0.0069 \leqslant 0.0069$ $\varepsilon_{fe,P}$ = 0.0037 < 0.0069	$\varepsilon_{fe,N} = 0.0069 \leqslant 0.0069$ $\varepsilon_{fe,P}$ = 0.0053 < 0.0069
9. Check tension steel strain	$\varepsilon_{s,N}$ = 0.0056 > 0.002 yield $\varepsilon_{s,P}$ = 0.0288 > 0.002 yield	$\varepsilon_{s,N}$ = 0.0056 > 0.002 yield $\varepsilon_{s,P}$ = 0.0394 > 0.002 yield
10–12. Factored flexural section capacity	$\phi_f M_{n,N}$ = 34.6 kN m $\phi_f M_{n,P}$ = 35.5 kN m	$\phi_f M_{n,N}$ = 37.0 kN m $\phi_f M_{n,P}$ = 36.2 kN m
13. Factored shear carrying capacity	$\phi_v V_n$ = 97.5 kN	$\phi_v V_n$ = 102.2 kN
14. Design factored load $w_u = \min(w_{u,P}, w_{u,N}, w_{u,V})$	w_u = 64.1 kN/m $w_{u,P}$ = 95.5 kN/m $w_{u,N}$ = 64.1 kN/m $w_{u,V}$ = 79.9 kN/m	w_u = 68.4 kN/m $w_{u,P}$ = 97.4 kN/m $w_{u,N}$ = 68.4 kN/m $w_{u,V}$ = 83.8 kN/m
15. Failure mode	As the left term of Eq. (8) 59.3 kN m is less than the right term 59.4 kN m, the failure mode is D-1 as shown in Fig. 12a	As the left term of Eq. (5) 61.7 kN m is less than the right term 62.3 kN m, the failure mode is D-1 as shown in Fig. 12b
16. Failure load Eq. (12) for failure mode D-1	w_f = 71.8 kN/m	w_f = 74.6 kN/m

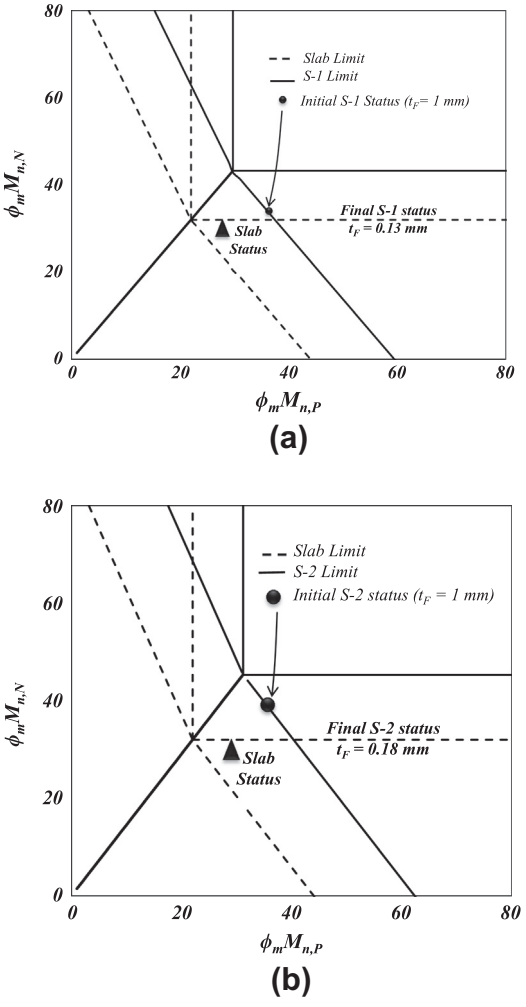

Fig. 12. The formulated failure limits and the estimated status of moment carrying capacities for the design example with (a) S-1 retrofit system and (b) S-2 retrofit system.

Table 7
Summary of the retrofit results using design examples.

Slabs	Failure mode	w_u (kN/m)	w_f (kN/m)	t_F (mm)
Existing slab	DB-1	52.7 [100%]	59.2 [100%]	–
Retrofit with S-1	D-1	64.1 [121%]	71.8 [121%]	0.13
Retrofit with S-2	D-1	68.4 [131%]	74.6 [126%]	0.18

ranged according to the debonding failure strain of CFRP as presented in Table 6. The steel stress level is determined at step 9, while the factored moment and shear capacities are determined in steps 10 through 13. The portion of the moment carrying capacity generated by CFRP is reduced by reliability factor of 0.85 [7] at step 12. In steps 14 through 16, the factored design load w_u and the failure load w_f are determined with the corresponding failure mode. At the first iteration of design in Table 5, for both S-1 system and S-2 system, w_u and w_f are governed by the shear strength of the slab with the B-1 failure mode. As shown in Fig. 12 for the initial retrofit status of both systems, the moment carrying capacity at the support section $\phi_m M_{n,N}$ is excessively enhanced and it will lead the retrofitted slabs to fail in shear even the delamination of CFRP is prevented. Therefore, by adjusting $\phi_m M_{n,N}$ of the retrofitted slab, which is governed by CFRP thickness, a ductile failure of the retrofitted slab can be attained. The final iterations of the design procedure with the optimal CFRP thickness are presented in Table 6. The final CFRP thickness will result in ductile D-1 failure mode for both S-1 system and S-2 overlay systems. It is noticeable that a ductile failure for the retrofitted slab can also be attained by increasing the shear strength limits of Eqs. (1) and (2) in Fig. 10. This can be achieved by increasing the shear strength of the HPC overlay.

The retrofitted slab capacities are summarized in Table 7. From this table, one can see that the hybrid retrofit systems of S-1 and S-2 have the efficiency to enhance the factored design load by 121% and 130% respectively. Moreover, the brittle failure mode DB-1 of the slab is retrofitted to a ductile failure mode D-1.

5. Conclusions

Failure modes of a continuous slab retrofitted with a hybrid system of FRP and HPC are evaluated according to moment and

shear carrying capacities. Realization of the failure modes enabled establishing design limits to ensure ductile flexural failure for the hybrid retrofit system. A methodology to determine the CFRP thickness to ensure ductile failure is demonstrated through a design example for retrofitting a continuous RC slab. It was also shown that the proposed system can convert the brittle shear failure of the unstrengthened slab to a ductile failure of the strengthened slab. Results of this study indicated that not only the hybrid retrofit system can provide enhancement of the factored design load up to 130%, but also it converts the brittle shear failure mode of the slab to a desirable ductile flexural failure mode.

Acknowledgements

Financial support to the first and second authors by the Human Resources Development of the Korea Institute of Energy Technology Evaluation and Planning (KETEP) Grant funded by the Korea government Ministry of Knowledge Economy (No. 20104010100520) is acknowledged. The experimental development program was part of the ICC-ES structural evaluation of the Linford, LLC composites system conducted at the ISO17025/IAS-Accredited Structural Engineering Test Hall (STEH) at the University of California, Irvine. The authors would like to extend their thanks to Linford, LLC for supplying and applying the LinTop® system.

References

[1] Mosalam KM, Mosallam AS. Nonlinear transient analysis of reinforced concrete slab subjected to blast loading and retrofitted with CFRP composites. Compos Part B: Eng 2001;32:623–36.
[2] Mosallam AS, Mosallam KM. Strengthening of two-way concrete slabs with FRP composite laminates. Constr Build Mater 2003;17:43–54.
[3] Nam J, Kim H, Kim S, Yi N, Kim JJ. Numerical evaluation of the retrofit effectiveness for GFRP retrofitted concrete slab subjected to blast pressure. Compos Struct 2010;92:1212–22.
[4] Fleming CJ, King GEM. The development of structural adhesives for three original uses in South Africa. In: RILEM international symposium, synthetic resins in building construction, Paris; 1967. p. 75–92.
[5] Emmons PH, Vaysburd AM, Thomas J. Strengthening concrete structure, Part II. Concr Int 1998;20(4):56–60.
[6] Rizkalla S, Hassan T, Hassan N. Design recommendations for the use of FRP for reinforcement and strengthening of concrete structures. Prog Struct Eng Mater 2003;5(1):16–28.
[7] ACI Committee 440. Guide for the design and construction of externally bonded FRP systems for strengthening concrete structures, ACI 440.2R-08, Farmington Hills, MI; 2008.
[8] Mosallam A, Reda Taha MM, Kim JJ, Nasr A. Strength and ductility of RC slabs strengthened with hybrid high-performance composite retrofit system. Eng Struct 2012;36:70–80.
[9] MacGregor JG, Wight JK. Reinforced concrete: mechanics and design. 5th ed. NJ, USA: Prentice Hall; 2009.
[10] ACI Committee 318. Building code requirements for structural concrete (ACI 318-05) and commentary (318R-05), American Concrete Institute, Farmington Hills, MI; 2005.
[11] Hognestad E. Study of combined bending and axial load in reinforced concrete members. University of Illinois, Bulletin Series, Bulletin 399; November 1951.
[12] Reed CE, Peterman RJ, Rasheed HA. Evaluating FRP repair method for cracked prestressed concrete bridge members subjected to repeated loadings (phase 1), KTRAN report, No. K-TRAN: KSU-01-2; 2005.